Institute of Space and Aeronautical Science, University of Tokyo
Report No. 447, March 1970

Measurement of the Wave Propagation by Correlation Techniques

By

Nobuharu AOSHIMA

Summary: Correlation techniques are used to measure the characterizing parameters of the wave propagation system. The traveling wave representation of a vibrating system is discussed. Delay times and amplitude coefficients are considered to be the characterizing parameters, not only in the nondispersive wave propagation system but also in the dispersive case, if group delay time is defined. Three kinds of correlation method, such as, the correlation envelope method, the squared signal correlation method and the *M*-sequence correlation method are proposed to measure the group delay time and wave intensity. The acoustic wave propagation as an example of nondispersive case and the flexural wave propagation as a dispersive case are described and typical measured correlation functions are illustrated.

1. INTRODUCTION

In considering wave propagation problem, the transfer function between two separate points will be a characteristic quantity of a linear system. For example, an exciting point of the vibration system is fixed and the space coordinate of the detecting point is assumed to be a variable parameter in the expression of the transfer function. From such transfer function, the response of the system for the arbitrary input signal can be obtained. But in many cases the expression of the transfer function would be complex form and the physical meaning is not clear or it is sometimes impossible to obtain the exact transfer function. In such a case it is desirable to get an approximate expression characterized by a few parameters whose physical meanings are clear, even if its validity is restricted in some narrow range of input signal.

The traveling wave representation of the transfer function is one of such approximate expressions. The input signal is assumed to travel as a few number of wave rays and the system characteristics are expressed by the delay times and amplitude coefficients of these wave rays. The correlation techniques are useful in measuring such parameters and some experiments have already been reported [*1*][*2*][*3*].

The delay time is defined when the signal waveform is not distorted, in other words, at the nondispersive wave propagation case. If the group delay time is defined, the same system characterization is possible for more general case, and correlation techniques are also applicable to measure the characterizing parameters.

These were reported by the author before [4]. The more general and detailed discussion of this topic will be made in this paper.

2. Phase Velocity and Group Velocity

The signal flow problem as Fig. 1 is considered. $G(s)$ is the transfer function of the linear system and the input and the output signal $f_1(t)$ and $f_2(t)$ are assumed to be bounded in amplitude and continuous and differentiable up to necessary order, and they can be represented as follows by choosing ω_n's suitably in the signal frequency range.

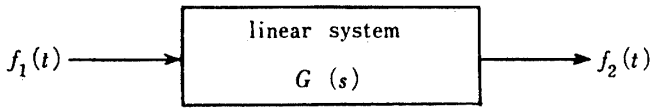

Fig. 1. Linear system.

$$f_1(t)=\sum_{n=1}^{N} C_n \cos(\omega_n t-\varphi_n) \tag{1}$$

$$f_2(t)=\sum_{n=1}^{N} C_n |G(i\omega_n)| \cos\{\omega_n t-\varphi_n+\angle G(i\omega_n)\} \tag{2}$$

When $G(s)$ has the form as

$$G(s)=\sum_{j=1}^{M} k_j e^{-s\tau_j} \tag{3}$$

then $f_2(t)$ is calculated as

$$f_2(t)=\sum_{j=1}^{M} k_j f_1(t-\tau_j) \tag{4}$$

This means that if the system transfer function can be expressed in the form as (3), the output signal $f_2(t)$ is represented as the superposition of input signal with some time delays and amplitude coefficients. If the expression of (3) is valid only for some particular input signal range, then the system characterization by time delays and amplitude coefficients is restricted in that range.

More generally, if $G(s)$ can be represented in some narrow frequency range, whose center angular frequency is ω_m,

$$\left.\begin{aligned} G(s)&=\sum_{j=1}^{M} G_j(s), & |G_j(i\omega)|&=k_j \\ -\frac{\angle G_j(i\omega)}{\omega}&=\tau_{mj}, & -\frac{d}{d\omega}\{\angle G_j(i\omega)\}&=\tau_{gj} \end{aligned}\right\} \tag{5}$$

then, for the arbitrary input signal whose frequency spectrum is confined in that frequency range, the relation of input and output signal is derived as

$$z_2(t)=\sum_{j=1}^{M} k_j z_1(t-\tau_{gj})\cdot\exp\{i\omega_m(\tau_{gj}-\tau_{mj})\} \tag{6}$$

where $z(t)$ is the pre-envelope of $f(t)$, and defined as

$$z(t)=f(t)+i\hat{f}(t) \tag{7}$$

$$\hat{f}(t)=\frac{1}{\pi}\int_{-\infty}^{\infty}\frac{f(\xi)}{t-\xi}d\xi \quad \text{(Hilbert transform of } f(t)\text{)} \tag{8}$$

The envelope of the signal is given as the absolute value of the pre-envelope. Then (6) is considered that the envelope of the output signal is represented as the sum of the envelope of the input signal with time delay τ_{gj} and amplitude coefficients k_j.

In the case of wave propagation, the group velocity and phase velocity are calculated from τ_g and τ_m respectively. The main purpose of this paper is the determination of parameters τ_{gj} and k_j in the equation (5) by theory and experiment.

3. Traveling Wave Representation of the Response of a Continuous System

One of the popular analyzing methods of vibration system is the modal analysis, in which the solution is obtained as the superposition of the eigenfunctions. Integral transform method such as Fourier or Laplace transforms is also used. There is the third method, which assumes the solution as the superposition of some traveling waves and adjust the coefficients of them to satisfy the initial and the boundary conditions. To make clear the meaning of such traveling wave representation, it will be shown that such solution can be derived analytically from the basic wave equation. Three examples are presented.

(1) *Longitudinal wave of finite bar*

Longitudinal motion of an uniform bar as Fig. 2 is considered. The wave equation is written as

$$\frac{\partial^2 u(x,t)}{\partial x^2}=\frac{1}{c^2}\frac{\partial^2 u(x,t)}{\partial t^2}, \quad c=\sqrt{\frac{EA}{m}}=\sqrt{\frac{E}{\rho}} \tag{9}$$

and the initial and the boundary conditions are assumed as

$$u(x,0)=\left.\frac{\partial u(x,t)}{\partial t}\right|_{t=0}=0 \tag{10}$$

$$u(0,t)=0, \quad EA\left.\frac{\partial u(x,t)}{\partial x}\right|_{x=L}=p(t) \tag{11}$$

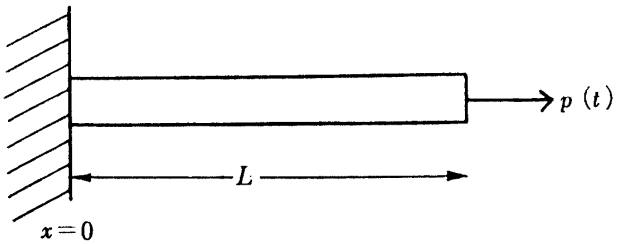

Fig. 2. Uniform bar in longitudinal motion.

where $u(x, t)$ is the longitudinal displacement, A is the cross section, E is the modulous of elasticity, ρ is the mass density and $p(t)$ is the force applied at the free end. $p(t)$ is regarded as the input signal and $u(x, t)$ is as the output signal and the transfer function is

$$G(x, s)=\frac{\bar{u}(x, s)}{\bar{p}(s)} \tag{12}$$

where $\bar{u}(x, s)$ and $\bar{p}(s)$ are the Laplace transform of $u(x, t)$ and $p(t)$ with respect to t.

To obtain the expression of (12), the Laplace transform of (9) with respect to t is derived taking into account the initial condition of (10) [5].

$$\frac{d^2\bar{u}(x, s)}{dx^2}-\left(\frac{s}{c}\right)^2\bar{u}(x, s)=0 \tag{13}$$

The transformed boundary conditions are

$$\bar{u}(0, s)=0, \quad EA\frac{d\bar{u}(x, s)}{dx}\bigg|_{x=L}=\bar{p}(s) \tag{14}$$

The solution of (13) and (14) is obtained as

$$\bar{u}(x, s)=\frac{c}{EA}\cdot\frac{\bar{p}(s)}{s}\cdot\frac{e^{(x/c)s}-e^{-(x/c)s}}{e^{(L/c)s}+e^{-(L/c)s}} \tag{15}$$

From this equation, $G(x, s)$ can be obtained at once as

$$G(x, s)=\frac{K}{s}\cdot\frac{e^{(x/c)s}-e^{-(x/c)s}}{e^{(L/c)s}+e^{-(L/c)s}}, \qquad K=\frac{c}{EA} \tag{16}$$

Now the problem is solved, but the physical meaning of the expression (16) is not clear, so it is rewritten as

$$G(x, s)=\frac{K}{s}e^{-(L/c)s}\cdot\frac{e^{(x/c)s}-e^{-(x/c)s}}{1+e^{-(2L/c)s}} \tag{17}$$

Since $Re\, s\geqq 0$, and $Re\, s=0$ is the limiting case, expanding the denominator of (17), it is written as

$$\begin{aligned} G(x, s)&=\frac{K}{s}e^{-(L/c)s}(e^{(x/c)s}-e^{-(x/c)s})(1-e^{-(2L/c)s}+e^{-(4L/c)s}-\cdots) \\ &=\frac{K}{s}(e^{-(L-x)s/c}-e^{-(L+x)s/c}-e^{-(3L-x)s/c}+e^{-(3L+x)s/c}+\cdots) \end{aligned} \tag{18}$$

This is the form of $G=\sum_j G_j$ and the first term is

$$G_1(x, s)=\frac{K}{s}e^{-(L-x)s/c} \tag{19}$$

$$-\frac{d}{d\omega}\{\angle G_1(x, i\omega)\}=\frac{L-x}{c} \tag{20}$$

$$|G_1(x, i\omega)| = \frac{K}{\omega} \tag{21}$$

If the input frequency range is restricted in narrow frequency band, (21) can be considered as constant, and the group delay time is given by (20), then it is clear that the first term represents the direct wave whose group velocity is c. The dependence of (21) on frequency is not intrinsic, for if instead of $u(x, t)$, its time derivative $(d/dt)u(x, t)$ is adopted as the output signal, ω vanishes from (21). In that case not only the group delay time but also the phase delay time is independent of frequency.

The second term of (18) is

$$G_2(x, s) = -\frac{K}{s} e^{-(L+x)s/c} \tag{22}$$

$$-\frac{d}{d\omega}\{\angle G_2(x, i\omega)\} = \frac{L+x}{c} \tag{23}$$

$$|G_2(x, i\omega)| = \frac{K}{\omega} \tag{24}$$

As (23) shows, (22) represents the wave reflected at $x=0$ and travels to positive x direction.

In the same way the third term represents the twice reflected wave and so on.

Thus the traveling wave representation (18) is derived analytically from the wave equation.

(2) *Bending motion of semi-infinite bar*

If the shear deformation and the rotatory inertia effects are neglected, the differential equation of bending motion of the uniform bar is

$$\frac{\partial^4 y(x, t)}{\partial x^4} + \frac{1}{a^2}\frac{\partial^2 y(x, t)}{\partial t^2} = 0, \qquad a^2 = \frac{EI}{m} \tag{25}$$

and the initial and the boundary conditions are assumed as

$$y(x, 0) = \left.\frac{\partial y(x, t)}{\partial t}\right|_{t=0} = 0 \tag{26}$$

$$y(0, t) = f(t), \qquad \left.\frac{\partial y(x, t)}{\partial x}\right|_{x=0} = 0 \tag{27}$$

The displacement at $x=0$ is thought to be input signal and that at the point $x>0$ is output signal. Considering that $y(x, s)$ must remain finite value for all positive x, the transfer function is obtained as

$$G(x, s) = \frac{1-i}{2} e^{(s/2a)^{1/2}(-1+i)x} + \frac{1+i}{2} e^{-(s/2a)^{1/2}(1+i)x} \tag{28}$$

The first term is

$$G_1(x, i\omega)=\frac{1-i}{2}e^{-(\omega/a)^{1/2}x} \tag{29}$$

$$-\frac{d}{d\omega}\{\angle G_1(x, i\omega)\}=0 \tag{30}$$

$$|G_1(x, i\omega)|=\frac{1}{\sqrt{2}}e^{-(\omega/a)^{1/2}x} \tag{31}$$

From (30), the wave propagates with no delay time but as (31) shows, its magnitude decreases exponentially and restricted to the immediate neighbors of the exciting point. This is known as the evanescent wave and its appearance is typical to the bending wave problem.

The second term is

$$G_2(x, i\omega)=\frac{1+i}{2}e^{-i(\omega/a)^{1/2}x} \tag{32}$$

$$-\frac{d}{d\omega}\{\angle G_2(x, i\omega)\}=\frac{x}{2(a\omega)^{1/2}} \tag{33}$$

$$|G_2(x, i\omega)|=\frac{1}{\sqrt{2}} \tag{34}$$

When the signal frequency is confined in the narrow range, (33) can be considered as constant, and this term represents the traveling wave with the group velocity $2(a\omega)^{1/2}$.

On the other hand, phase delay time of (32) is calculated as

$$-\frac{\angle G_2(x, i\omega)}{\omega}=\frac{\pi}{4\omega}+\frac{x}{(a\omega)^{1/2}} \tag{35}$$

The second term is the intrinsic part to the wave propagation, and the phase velocity is given as $(a\omega)^{1/2}$, which is half of the group velocity.

(3) *Bending motion of finite bar*

A finite bar with length L is examined. The differential equation is (25) and the boundary conditions are in addition to (27)

$$\left.\frac{\partial^2 y(x, t)}{\partial x^2}\right|_{x=L}=\left.\frac{\partial^3 y(x, t)}{\partial x^3}\right|_{x=L}=0 \tag{36}$$

These are the free end conditions at $x=L$. The initial conditions are the same as (26). Then the transfer function is calculated as

$$G(x, s)=\frac{|M(x)|}{|M(0)|}=\sum_{j=1}^{4}\frac{\Delta_{1j}}{|M(0)|}e^{A_j x} \tag{37}$$

where

$$M(x)=\begin{bmatrix} e^{A_1x} & e^{A_2x} & e^{A_3x} & e^{A_4x} \\ A_1 & A_2 & A_3 & A_4 \\ A_1^2e^{A_1L} & A_2^2e^{A_2L} & A_3^2e^{A_3L} & A_4^2e^{A_4L} \\ A_1^3e^{A_1L} & A_2^3e^{A_2L} & A_3^3e^{A_3L} & A_4^3e^{A_4L} \end{bmatrix} \tag{38}$$

$$A_j=\sqrt{\frac{s}{a}}e^{(\pi/4)(2j-1)i}, \qquad j=1\sim 4 \tag{39}$$

and Δ_{1j}'s are the $(1, j)$ cofactors of M.
The first term of (37) is

$$G_1(x, s)=\frac{\Delta_{11}}{|M(0)|}e^{A_1x}=\frac{\{(1-i)e^{-2iBL}+(1+i)e^{-2BL}+2\}e^{A_1x}}{2e^{-2iBL}+2e^{2iBL}+2e^{-2BL}+2e^{2BL}+8} \tag{40}$$

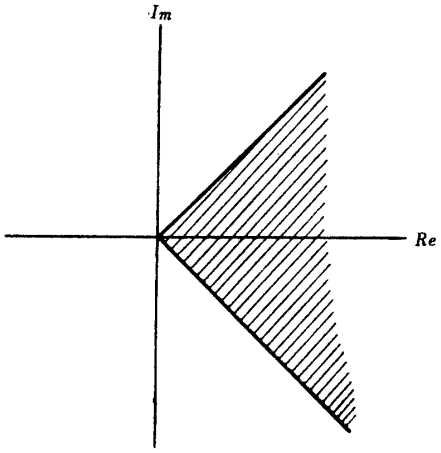

FIG. 3. The range of $B=(s/2a)^{1/2}$.

Since $Re\, s>0$, $B=(s/2a)^{1/2}$ must be in the hatched area of Fig. 3, and e^{2BL} is larger than the sum of the other terms in denominator in absolute value, when L is large enough. In such case, expanding the denominator, $G_1(x, s)$ is written as

$$\begin{aligned} G_1(x, s)&=e^{A_1x-2BL}\left\{1+\frac{1-i}{2}e^{-2iBL}+\frac{1+i}{2}e^{-2BL}\right\} \\ &\quad\times\{1-e^{-2iBL-2BL}-e^{2iBL-2BL}-e^{-4BL} \\ &\quad-4e^{-2BL}+\cdots\} \\ &=e^{A_1x-2BL}+\frac{1-i}{2}e^{A_1x-2BL-2iBL} \\ &\quad-\frac{1-i}{2}e^{A_1x-4BL-4iBL}+\cdots \end{aligned} \tag{41}$$

The first term of (41) is

$$G_{11}(x, i\omega)=e^{(\omega/a)^{1/2}xi-(\omega/a)^{1/2}L(1+i)} \tag{42}$$

$$-\frac{d}{d\omega}\{\angle G_{11}(x, i\omega)\}=\frac{L-x}{2(a\omega)^{1/2}} \tag{43}$$

$$|G_{11}(x, i\omega)|=e^{-(\omega/a)^{1/2}L} \tag{44}$$

When $|e^{2BL}|$ is large, it means $\omega^{1/2}L$ is large and as (44) shows this term is almost zero. The second term of (41) is

$$G_{12}(x, i\omega)=\frac{1-i}{2}e^{(\omega/a)^{1/2}(x-2L)i} \tag{45}$$

$$-\frac{d}{d\omega}\{\angle G_{12}(x, i\omega)\}=\frac{2L-x}{2(a\omega)^{1/2}} \tag{46}$$

$$|G_{12}(x, i\omega)| = \frac{1}{\sqrt{2}} \tag{47}$$

As (46) shows, this term represents the traveling wave reflected at $x=L$ and propagates to the negative x direction with the group velocity $2(a\omega)^{1/2}$. As the same way the third term of (41) is shown to represent the twice reflected wave at $x=L$. When the exponent of each term of (41) is written as $-\alpha BL - i\beta BL$, it stands generally that $\alpha \geqq \beta$. When $\alpha > \beta$ the corresponding terms vanish and when $\alpha = \beta$ they remain and represent the wave traveling negative x direction.

The second term of (37) is

$$G_2(x, s) = e^{A_2 x - 2BL} + \frac{1-i}{2} e^{A_2 x} + \frac{1+i}{2} e^{A_2 x - 2BL - 2iBL} + \cdots \tag{48}$$

The first term of (48) is

$$G_{21}(x, i\omega) = e^{-(\omega/a)^{1/2} x - (\omega/a)^{1/2} L(1+i)} \tag{49}$$

$$|G_{21}(x, i\omega)| = e^{-(\omega/a)^{1/2}(x+L)} \tag{50}$$

(50) shows this term is almost zero. The second term is

$$G_{22}(x, i\omega) = \frac{1-i}{2} e^{-(\omega/a)^{1/2} x} \tag{51}$$

$$-\frac{d}{d\omega}\{\angle G_{22}(x, i\omega)\} = 0 \tag{52}$$

$$|G_{22}(x, i\omega)| = \frac{1}{\sqrt{2}} e^{-(\omega/a)^{1/2} x} \tag{53}$$

These are the same form as (29)–(31), and represent the evanescent wave generated at $x=0$. The third term of (48) is

$$G_{23}(x, i\omega) = \frac{1+i}{2} e^{-(\omega/a)^{1/2}(x+2Li)} \tag{54}$$

$$-\frac{d}{d\omega}\{\angle G_{23}(x, i\omega)\} = \frac{2L}{2(a\omega)^{1/2}} \tag{55}$$

$$|G_{23}(x, i\omega)| = \frac{1}{\sqrt{2}} e^{-(\omega/a)^{1/2} x} \tag{56}$$

This is the evanescent wave at $x=0$, which is generated, as (55) shows, by the wave that propagates to the far end and reflected back to $x=0$. In the same way the evanescent waves generated by multiply reflected traveling waves are introduced and other terms of (48) vanish.

The third term $G_3(x, s)$ and fourth term $G_4(x, s)$ of (37) are shown in the same way as above to represent respectively the traveling waves to the positive x direction and the evanescent waves generated at $x=L$.

4. Correlation Techniques for the Wave Propagation Measurement

Correlation techniques are useful in measuring signal delay times and intensities. Auto- and cross-correlation function are defined as follows

$$\phi_x(\tau)=\overline{x(t)\cdot x(t+\tau)}, \qquad \phi_{xy}(\tau)=\overline{x(t)\cdot y(t+\tau)} \tag{57}$$

where upper bar means to take average with respect to t.

If the system transfer function is written as (3), the output signal $f_2(t)$ is expressed as (4), and the cross-correlation function of input and output signal is derived as

$$\phi_{f_1f_2}(\tau)=\sum_{j=1}^{M} k_j\phi_{f_1}(\tau-\tau_j) \tag{58}$$

From (58), if the autocorrelation function $\phi_{f_1}(\tau)$ is known, the delay time τ_j and the amplitude coefficient k_j can be measured. Especially if $\phi_{f_1}(\tau)$ is nearly zero when $|\tau|>T$, then for $|\tau_i-\tau_j|>T$ $(i\neq j)$, each term of (58) does not superpose and τ_j and k_j can be detected easily.

When $G(s)$ has more general form as (5), correlation methods are also applicable and as the delay time, the group delay is measured. This was discussed in a previous paper [4], and three methods of correlation measurement were proposed. They will be explained in the following in more general form.

(1) *Correlation envelope method*

When the system transfer function has the form as (5), the pre-envelope of the output signal is written as (6), and the cross-correlation function of the complex values $z_1(t)$ and $z_2(t)$ is calculated as

$$\begin{aligned}\phi_{z_1z_2}(\tau)&=\overline{z_1^*(t)\cdot z_2(t+\tau)}\\&=\sum_{j=1}^{M} k_j\phi_{z_1}(\tau-\tau_{gj})\exp\{i\omega_m(\tau_{gj}-\tau_{mj})\}\end{aligned} \tag{59}$$

where the asterisk means to take complex conjugate.
There are another relations [4].

$$\phi_{z_1}(\tau)=2\{\phi_{f_1}(\tau)+i\hat{\phi}_{f_1}(\tau)\}=2S_1(\tau)e^{iP_1(\tau)} \tag{60}$$

$$\phi_{z_1z_2}(\tau)=2\{\phi_{f_1f_2}(\tau)+i\hat{\phi}_{f_1f_2}(\tau)\}=2S_2(\tau)e^{iP_2(\tau)} \tag{61}$$

where $S(\tau)$ is the envelope and $P(\tau)$ is the phasing function of $\phi(\tau)$.
From (59), (60) and (61)

$$S_2(\tau)e^{iP_2(\tau)}=\sum_{j=1}^{M} k_jS_1(\tau-\tau_{gj})\exp\{iP_1(\tau-\tau_{gj})+i\omega_m(\tau_{gj}-\tau_{mj})\} \tag{62}$$

If $S_1(\tau)=0$ when $|\tau|>T$, and $|\tau_{gi}-\tau_{gj}|>T$ $(i\neq j)$, then each term of (62) does not superpose, and by taking absolute value

$$S_2(\tau)=\sum_{j=1}^{M} k_j S_1(\tau-\tau_{gj}) \tag{63}$$

When random signal is used as the input signal, $S_1(\tau)$ is almost zero when $|\tau|$ is large, so (63) means that from the envelope of the cross-correlation function, the group delay times τ_{gj} and the amplitude coefficients k_j can be measured.

(2) *Squared signal correlation method*

Measuring system is shown in Fig. 4. The output of the low pass filter is given as [4]

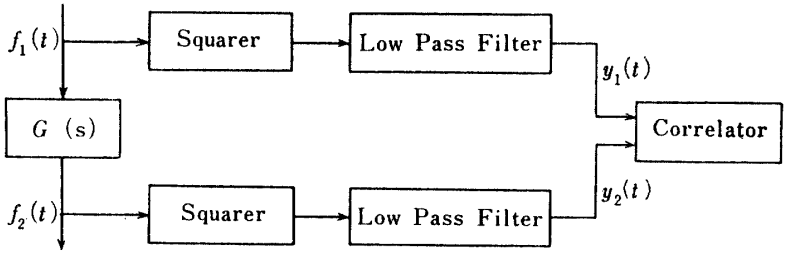

FIG. 4. Measuring system by squared signal correlation method.

$$y(t)=\frac{1}{2}|z(t)|^2 \tag{64}$$

When the system transfer function is written as (5), the pre-envelope of the output signal is expressed as (6), and $y_2(t)$ is obtained as

$$\begin{aligned} y_2(t)=&\frac{1}{2}\sum_j\sum_l k_j k_l z_1(t-\tau_{gj})\cdot z_1^*(t-\tau_{gl}) \\ &\times\exp\{i\omega_m(\tau_{gj}-\tau_{mj})-i\omega_m(\tau_{gl}-\tau_{ml})\} \end{aligned} \tag{65}$$

Then $\phi_{y_1y_2}(\tau)$ is written as

$$\begin{aligned} \phi_{y_1y_2}(\tau)=&\frac{1}{2}\sum_j\sum_l k_j k_l \overline{z_1(t+\tau-\tau_{gj})\cdot z_1^*(t+\tau-\tau_{gl})\cdot\frac{1}{2}|z_1(t)|^2} \\ &\times\exp\{i\omega_m(\tau_{gj}-\tau_{mj})-i\omega_m(\tau_{gl}-\tau_{ml})\} \end{aligned} \tag{66}$$

When $f_1(t)$ is random signal whose mean value is zero, then $z_1(t)$ is also zero mean random signal and it is considered that

$$\overline{z_1(t+\tau-\tau_{gj})\cdot z_1^*(t+\tau-\tau_{gl})\cdot|z_1(t)|^2}$$

is almost zero when $|\tau_{gj}-\tau_{gl}|$ is large. Then the terms of $j\neq l$ in (66) vanish, and

$$\phi_{y_1y_2}(\tau)=\frac{1}{4}\sum_{j=1}^{M} k_j^2\overline{|z_1(t+\tau-\tau_{gj})|^2\cdot|z_1(t)|^2}=\sum_{j=1}^{M}\frac{k_j^2}{4}\phi_{R_1^2}(\tau-\tau_{gj}) \tag{67}$$

where $\phi_{R_1^2}(\tau)$ is the autocorrelation function of the square of the envelope of $f_1(t)$. (67) means that by computing the cross-correlation function of $y_1(t)$ and $y_2(t)$, τ_{gj}

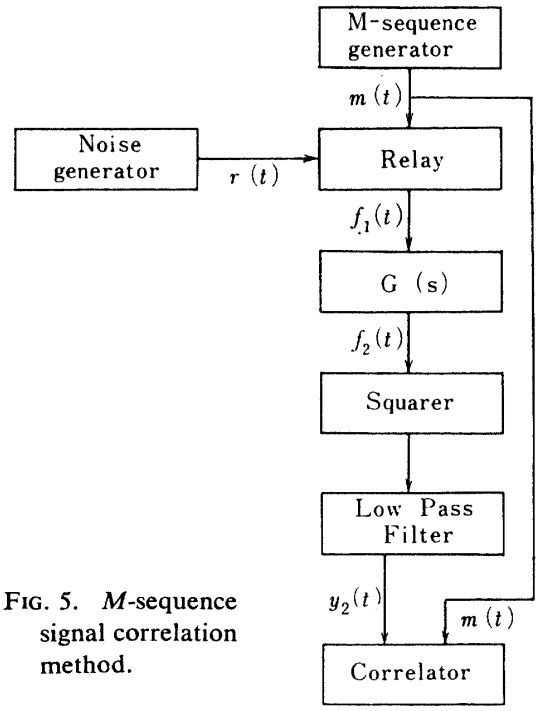

FIG. 5. *M*-sequence signal correlation method.

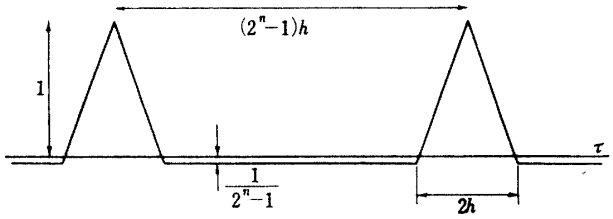

FIG. 6. Autocorrelation function of *M*-sequence signal.

and k_j^2 can be measured.

(3) *M-sequence signal correlation method*

Measuring system is shown in Fig. 5. As an input signal $f_1(t)$, band noise $r(t)$ intermitted by an *M*-sequence signal $m(t)$ is used. It is expressed as

$$f_1(t)=\frac{1}{2}\{m(t)+1\}r(t)=m'(t)\cdot r(t), \tag{68}$$
$$m(t)=+1 \text{ or } -1$$
$$m'(t)=\frac{1}{2}\{m(t)+1\}$$

M-sequence (Maximum period null sequence) signal is a two-valued pseudo-random artificial signal whose autocorrelation is given as Fig. 6. h is the time unit and n is the order of the *M*-sequence.

When the system transfer function is written as (5), $y_2(t)$ is written as (65), and the cross-correlation of $m(t)$ and $y_2(t)$ is expressed as

$$\phi_{my_2}(\tau)=\frac{1}{2}\sum_j\sum_l k_j k_l \overline{z_1(t+\tau-\tau_{gj})\cdot z_1^*(t+\tau-\tau_{gl})\cdot m(t)}$$
$$\times\exp\{i\omega_m(\tau_{gj}-\tau_{mj})-i\omega_m(\tau_{gl}-\tau_{ml})\} \tag{69}$$

Since $r(t)$ is a random singnal, it is considered that when $|\tau_{gj}-\tau_{gl}|$ is large, $\overline{z_1(t+\tau-\tau_{gj})\cdot z_1^*(t+\tau-\tau_{gl})\cdot m(t)}$ is almost zero. Then

$$\phi_{my_2}(\tau)=\frac{1}{2}\sum_{j=1}^{M} k_j^2\,\overline{|z_1(t+\tau-\tau_{gj})|^2\cdot m(t)} \tag{70}$$

It is derived that [4]

$$|z_1(t)|=m'(t)\cdot R_r(t) \tag{71}$$

where $R_r(t)$ is the envelope of $r(t)$. Then

$$\phi_{my_2}(\tau)=\frac{1}{2}\sum_{j=1}^{M} k_j^2\,\overline{R_r^2(t+\tau-\tau_{gj})\cdot m'^2(t+\tau-\tau_{gj})\cdot m(t)}$$
$$=\frac{1}{2}\sum_{j=1}^{M} k_j^2\,\overline{R_r^2(t+\tau-\tau_{gj})}\cdot\overline{m'(t+\tau-\tau_{gj})\cdot m(t)}$$
$$(\because\quad m'^2(t)=m'(t),\ \text{since } m'(t) \text{ is 0 or 1})$$

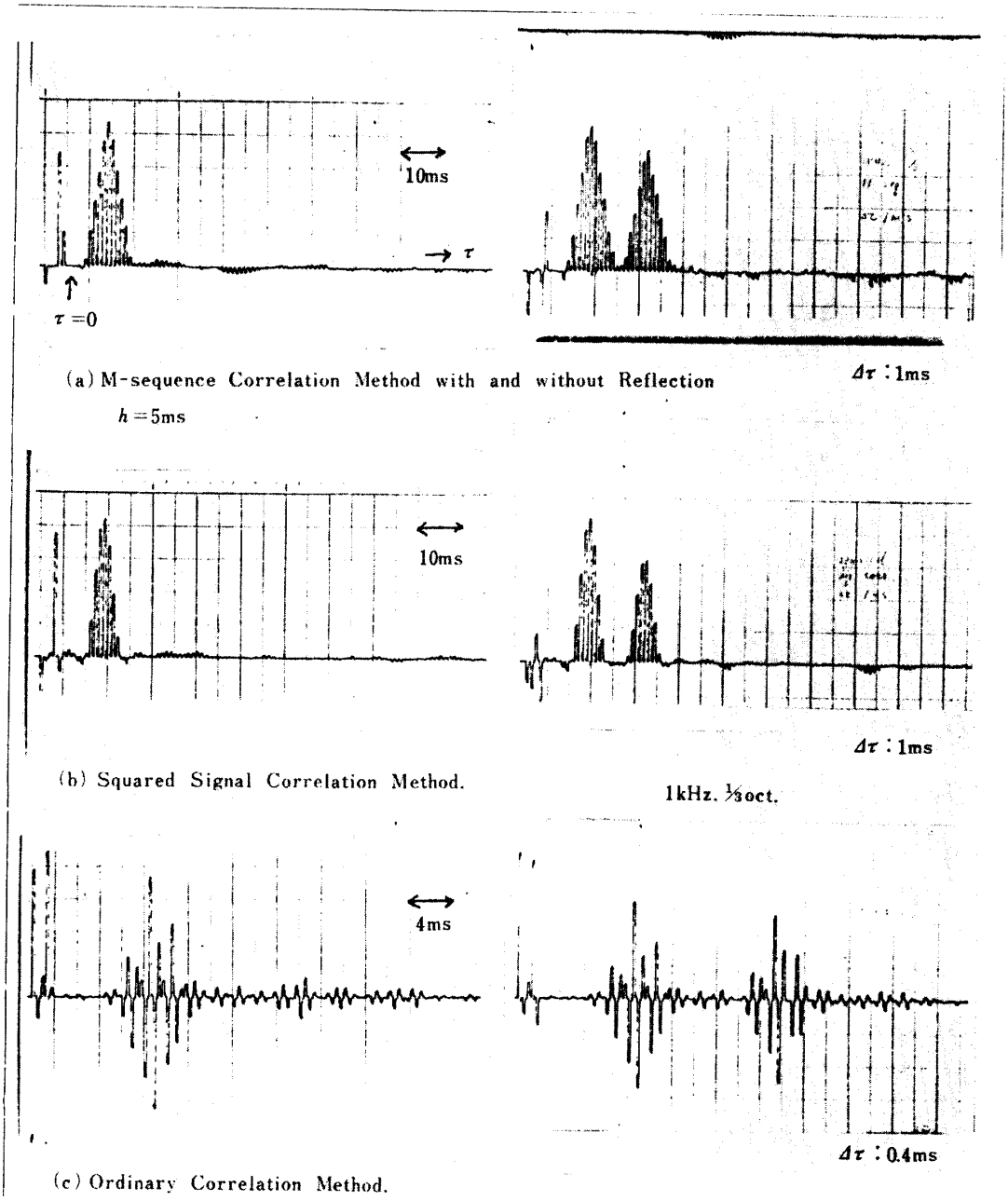

(a) M-sequence Correlation Method with and without Reflection

(b) Squared Signal Correlation Method.

(c) Ordinary Correlation Method.

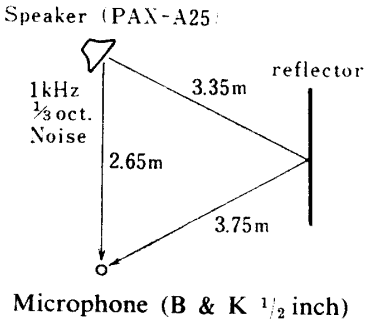

FIG. 7. Three methods of correlation Measurement. 1 kHz 1/3 octave band noise.

$$= \sum_{j=1}^{M} \frac{k_j^2}{2} \phi_r(0) \cdot \phi_m(\tau - \tau_{gj}) \tag{72}$$

In the above derivation the average of $m(t)$ is considered as zero. From (72), τ_{gj} and k_j^2 can be measured.

The power spectrum of $f_1(t)$ is almost equal to the power spectrum of $r(t)$, if the time unit h of the M-sequence signal is sufficiently large, so the M-sequence correlation method is very useful in measuring the propagation properties of waves by varying the signal frequency band.

5. Experiments

The acoustic wave propagation is an example of nondispersive wave propagation, in which the group velocity is equal to the phase velocity. The results of three methods of correlation measurements, those are (a) M-sequence method, (b) squared signal method and (c) ordinary correlation method are shown in Fig. 7. The speaker, the microphone and the reflecting board are placed in the anechoic room and the propagation of 1/3 octave band noise whose center frequency is 1 kHz is measured. As a squarer, Burr-Brown's squaring module 9875/19 is used. The sampling values of the computed cross-correlation functions are recorded on the chart of a pen-writing recorder [6][7]. The sampling interval is 1 millisecond in the cases of (a) and (b), but 0.4 ms in (c), because of the sampling theorem, it is impossible to represent the ordinary correlation function of 1 kHz signal by 1 ms sampling interval. The measurement of 5 kHz 1/3 octave band noise is shown in Fig. 8. In this case the ordinary correlation method can not be applied, for the minimum sampling interval of the correlator which is used in this study is 0.2 ms. The results when the reflecting board is removed are shown in the left of each measurement. As the figure shows, the cross-correlation functions by the M-sequence method are triangular form and do not depend on the signal frequency and it is easier to detect the delay time and the peak height compaired with other methods.

In Fig. 9, the cross-correlation functions obtained by M-sequence method are shown as a function of the distance from the speaker to the microphone. In these measurements the input signal to the speaker is added to the output of the microphone as shown in the figure. The correlation peak at $\tau=0$ corresponds to this signal and serves as the reference height to the correlation peaks. By this technique, the fluctuation of the signal source does not affect the results and the integrating number of the correlator can be changed arbitrary. The measurement is made by 5 kHz 1/3 octave band noise modulated by the M-sequence signal whose time unit is 1 ms, and the sampling interval of the correlator is 0.2 ms. The amplifier gain of the microphone output is increased 10 dB in the case (e)-(i). The measured delay times and intensities are plotted in Fig. 10. From Fig. 10(a) the sound velocity is obtained as 341 m/s. The temperature when the measurement was performed was in the range of 19°C–20°C, so the theoretical value is calculated as

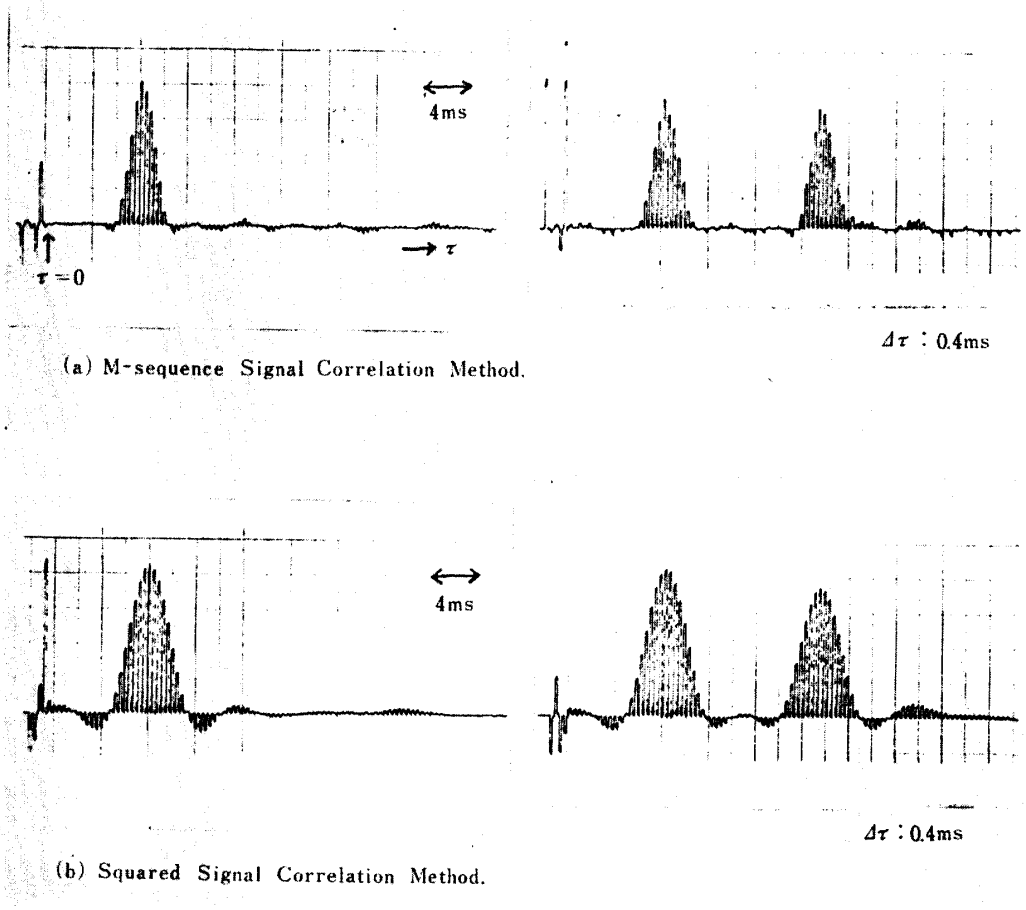

FIG. 8. *M*-sequence method and squared signal method. 5 kHz 1/3 oct. band. (Ordinary correlation method can not be applied in this case)

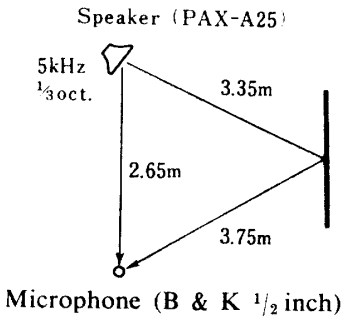

343 m/s. From Fig. 10(b) it is seen that the intensity of sound decreases 5.9 dB for doubling the distance, which is almost equal to 6.0 dB. These results assure the *M*-sequence correlation method is accurate enough in acoustic measurements. Some applications are reported in [3].

As an example of dispersive wave, the flexural wave in solid body is measured. Its phase velocity is given as

$$v_p=(EI/A\rho)^{1/4}\omega^{1/2} \tag{73}$$

and the group velocity is

$$v_g=2(EI/A\rho)^{1/4}\omega^{1/2}=2v_p \tag{74}$$

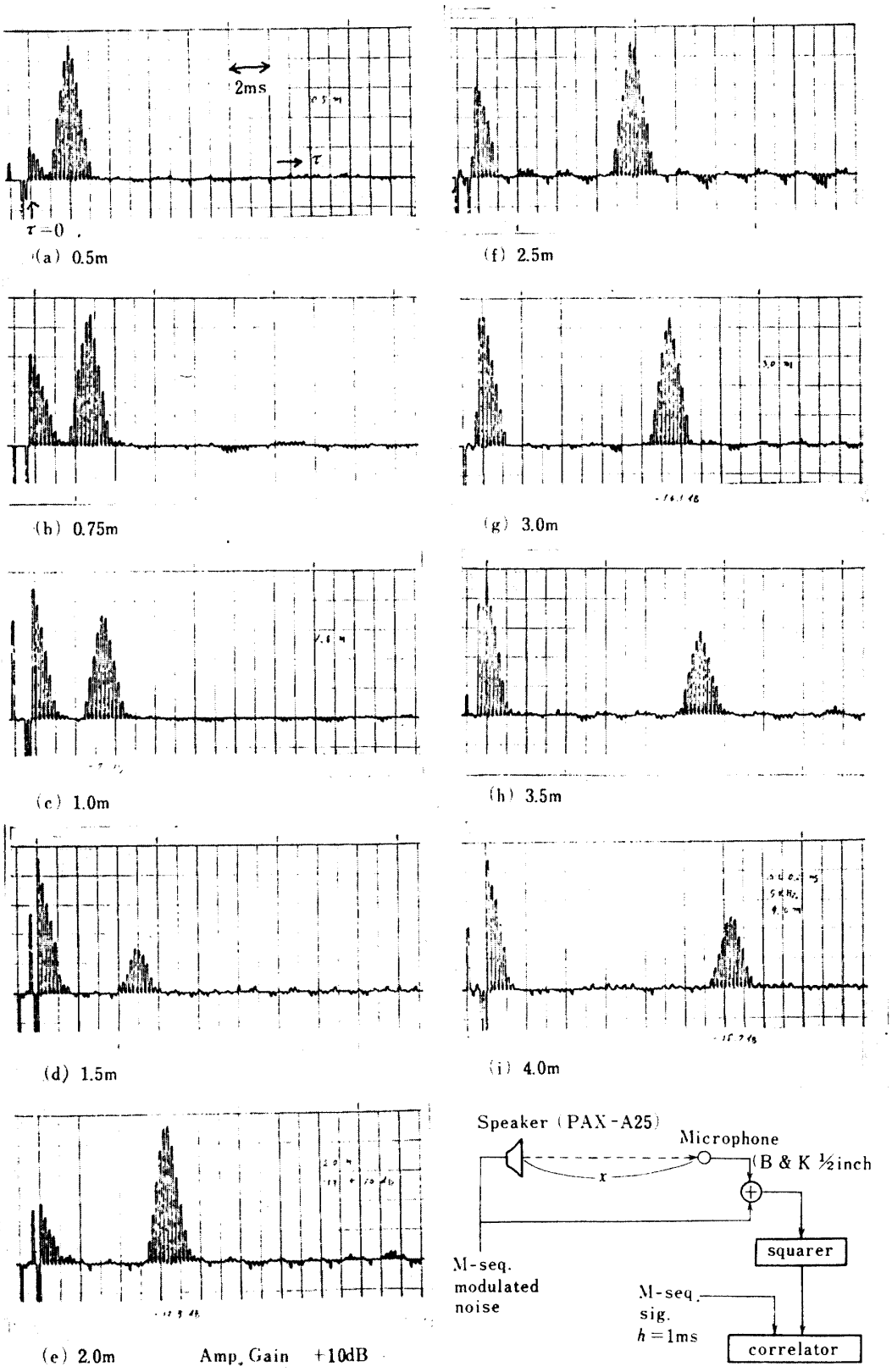

FIG. 9. Sound propagation. 5 kHz 1/3 oct.

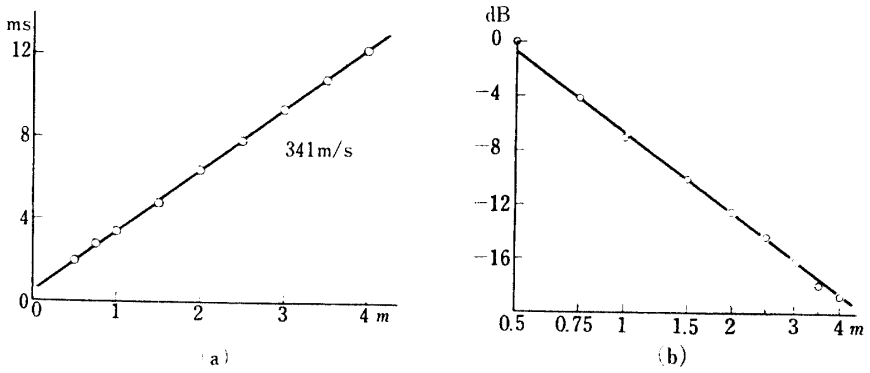

FIG. 10. (a) Time delay and (b) Intensity of sound. 5 kHz 1/3 oct.

where E is Young's modulous, I is moment of inertia of a section, A is a cross section and ρ is the density of the material. A long thin steel strip whose cross section is 0.75×38.2 mm is suspended by the strings horizontally, and the flexural wave is excited by an electromagnet. The wave is detected by a piezoelectric vibration pick-up whose weight is 1 gram and frequency response is from 2 Hz to 20 kHz within 1 dB. The measuring setup and obtained correlation functions are shown in Fig. 11. The steel strip is bended in the middle and both ends are suppressed by oil-treated cray. The reflected waves do not appear in the correlation records, for they are out of the range of delay time. The test signal is 1/3 octave band noise centered at 8 kHz, which is narrow enough to travel a few meters without serious distortion. The delay time versus distance is plotted in Fig. 12, from which the group velocity is obtained as 455 m/s. The same measurements are performed varying the signal frequency from 0.5 to 10 kHz and the results are plotted in Fig. 13. From this figure the relation $v=5.2\sqrt{f}$ is obtained when v is measured by m/s and f is by Hz. The theoretical relation calculated from the thickness, Young's modulous and density of steel is $v=5.28\sqrt{f}$.

In the above measurement the results are independent of the wave strength. To measure the wave strength, two pick-ups are used, one as a standard. The setup and one of the results are shown in Fig. 14. To separate two correlation peaks when the distance of the pick-ups is small, the output of pick-up 1 is transformed to sound ray in the anechoic room and dummy time delay of about 15 ms is introduced. This technique is useful to compare the wave intensities at the points nearby. From theoretical consideration of end excited flexural wave in lossless semi-infinite bar, the vibration velocity u is written as $u(x)=a(e^{-ikx}+e^{-kx})$ where u is complex value and time dependent factor $e^{i\omega t}$ is omitted. u satisfies the equation $d^4u/dx^4-k^4u=0$ and the free end boundary condition, that is the bending moment is zero at the end. The vibration intensity is expressed by the quantity

$$I_u(x)=\frac{1}{2}u\cdot u^*=\frac{1}{2}|a|^2(1+2e^{-kx}\cos kx+e^{-2kx}) \tag{75}$$

which is expected to correspond to the height of the correlation peak. The second and the third terms are the evanescent waves and their influence is restricted to the immediate neighbor of $x=0$. But at $x=0$ the relation

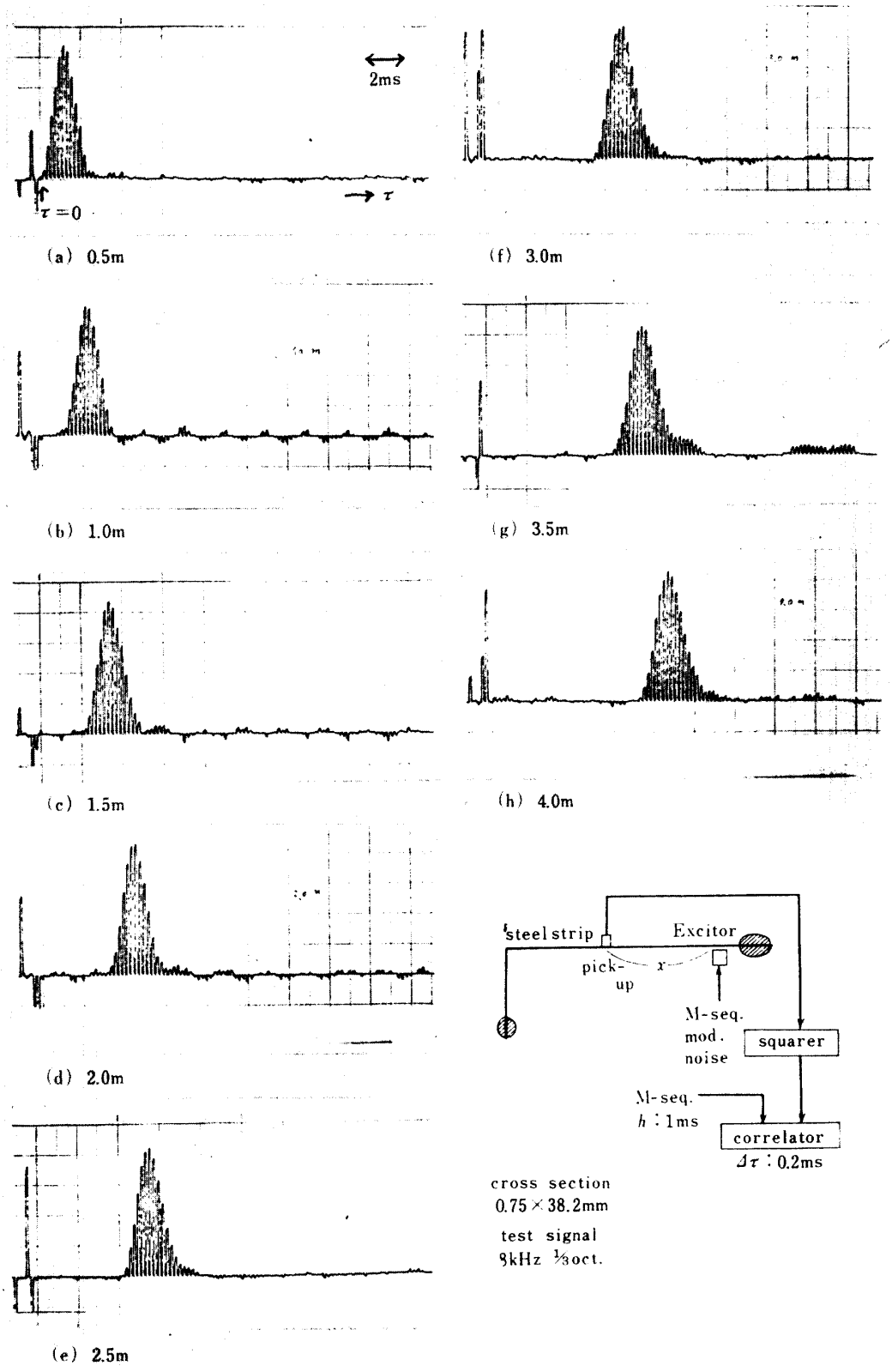

FIG. 11. Flexural wave propagation.

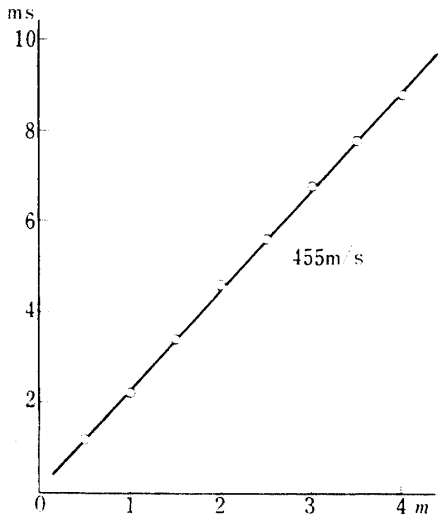

FIG. 12. Flexural wave propagation. 8 kHz 1/3 oct. 0.75 mm thickness steel.

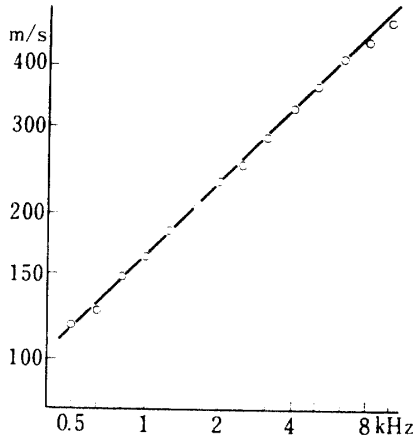

FIG. 13. Flexural wave propagation. Group velocity vs. frequency.

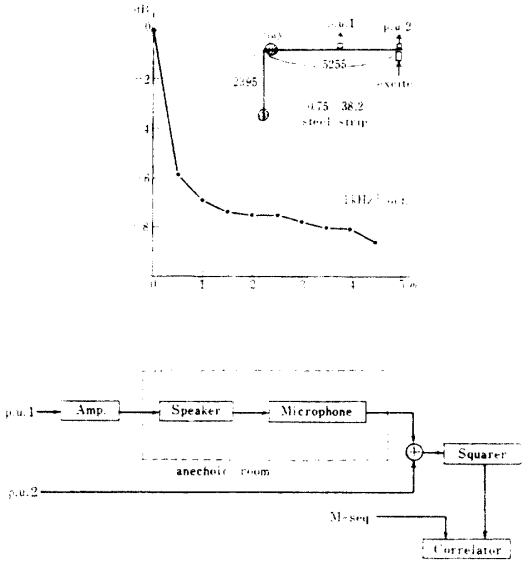

FIG. 14. Flexural wave excited at the free end.

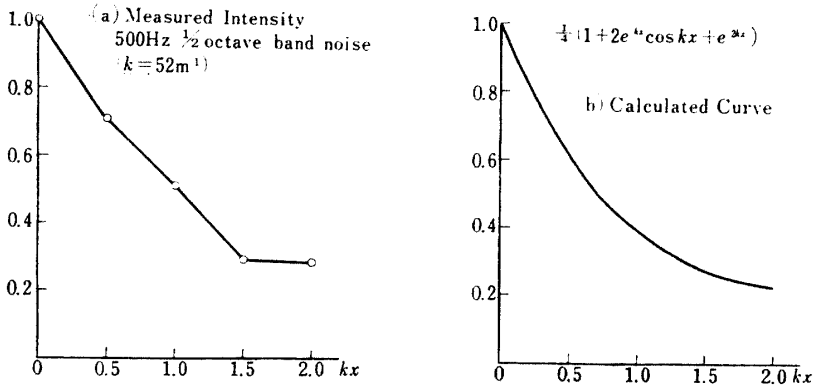

FIG. 15. Flexural wave near the free end.

$$I_u(0)/I_u(\infty)=4 \tag{76}$$

is derived, which corresponds to the result in Fig. 14 that the value at $x=0$ is almost 6 dB higher than the value at $x=0$ exterpolated from other values. The detailed measurements near the free end are shown in Fig. 15(a) and for comparison the calculated curve from (75) is shown in Fig. 15(b). The measurement is made by 500 Hz 1/2 octave band noise and the calculation is for the sinusoidal excitation case, but the correspondence of two graphs is good.

Next, the excitor is placed at the point 5.0 m apart from the free end and the reflection at the free end is measured. The setup and one of the results are shown in Fig. 16. This time the measurement is made at three points in the direction of width for each distance, which are grouped in the figure. Five correlation peaks are observed and each of them corresponds to, from left to right, the direct wave to p.u.1, the direct wave to p.u.2, the reflected wave to p.u.2, the reflected wave to p.u.1 and the twice reflected wave to p.u.2. The correlation function in (h) is the case when p.u.2 is removed. This is the case of 1 kHz 1/3 octave band noise. Varying signal frequency from 500 Hz to 2 kHz by 1/3 octave step, the measurements were performed and the heights of second and third peaks in reference to the first peak as a standard, are plotted in Fig. 17. From the theoretical consideration of the free end reflection of the sinusoidal wave in semi-infinite bar, the vibration velocity as a function of position is obtained as

$$u(x)=a\{e^{-ikx}+ie^{ikx}+(1+i)e^{-kx}\} \tag{77}$$

and the intensity of vibration is

$$I_u(x)=\frac{u\cdot u^*}{2}=|a|^2(1-\sin 2kx+2e^{-kx}\cos kx-2e^{-kx}\sin kx+e^{-2kx}) \tag{78}$$

As the distance x is becoming large this quantity oscillates between 0 and $2|a|^2$ by the effect of interference, but when the random signal is used, the strength of the incident and reflected wave would be $|a|^2/2$. On the other hand $I_u(0)=4|a|^2$, so at the free end the strength of vibration is 8 times of the incident wave. This consideration is verified as shown in Fig. 17, though the increment at the free end is rather small. As for the attenuation it is known that Q is substantially independent of frequency in the vibration of solid body, and spatial attenuation factor is given as $\exp(-\alpha x)$ where $\alpha=\omega/2cQ$. From this relation it is derived that the intensity of the wave decreases 8.68 α dB per meter, which is proportional to the square root of frequency [8]. The measured values in Fig. 17 vary widely and an accurate value of attenuation can not be expected, but the approximate values 0.3–0.8 dB/m and the tendency of increasing attenuation with frequency is observed.

Next, the reflection and the transmission at a right angle bend are measured. The setup and the results are shown in Fig. 18. The reflected waves are seen in the lower parts, and the values at more than 5 m correspond to transmitted waves beyond the bend. From the theoretical consideration of the wave reflection at the right angle bend, it is derived that when the flexural wave velocity is small enough

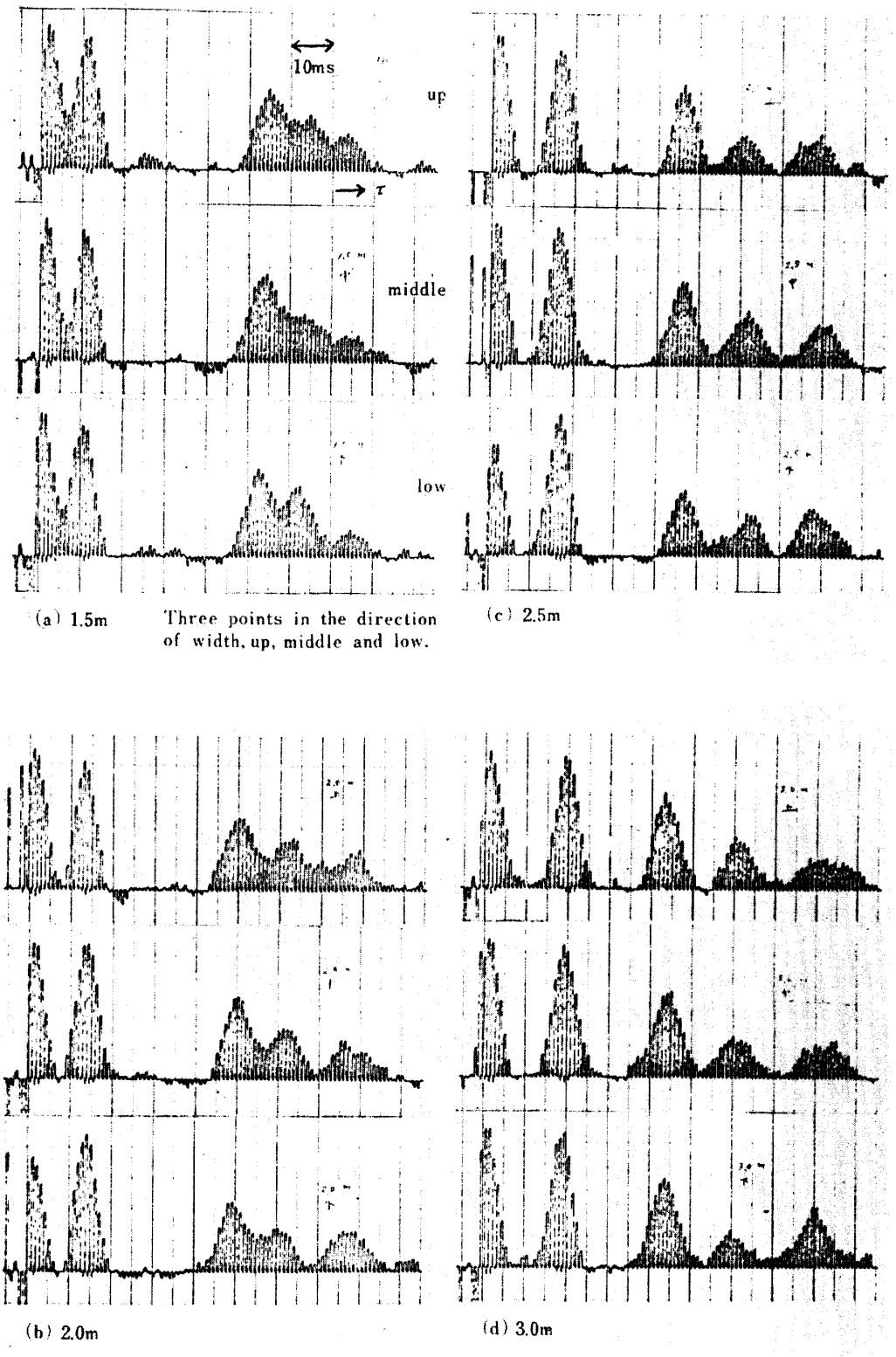

(a) 1.5m Three points in the direction of width, up, middle and low. (c) 2.5m

(b) 2.0m (d) 3.0m

FIG. 16.

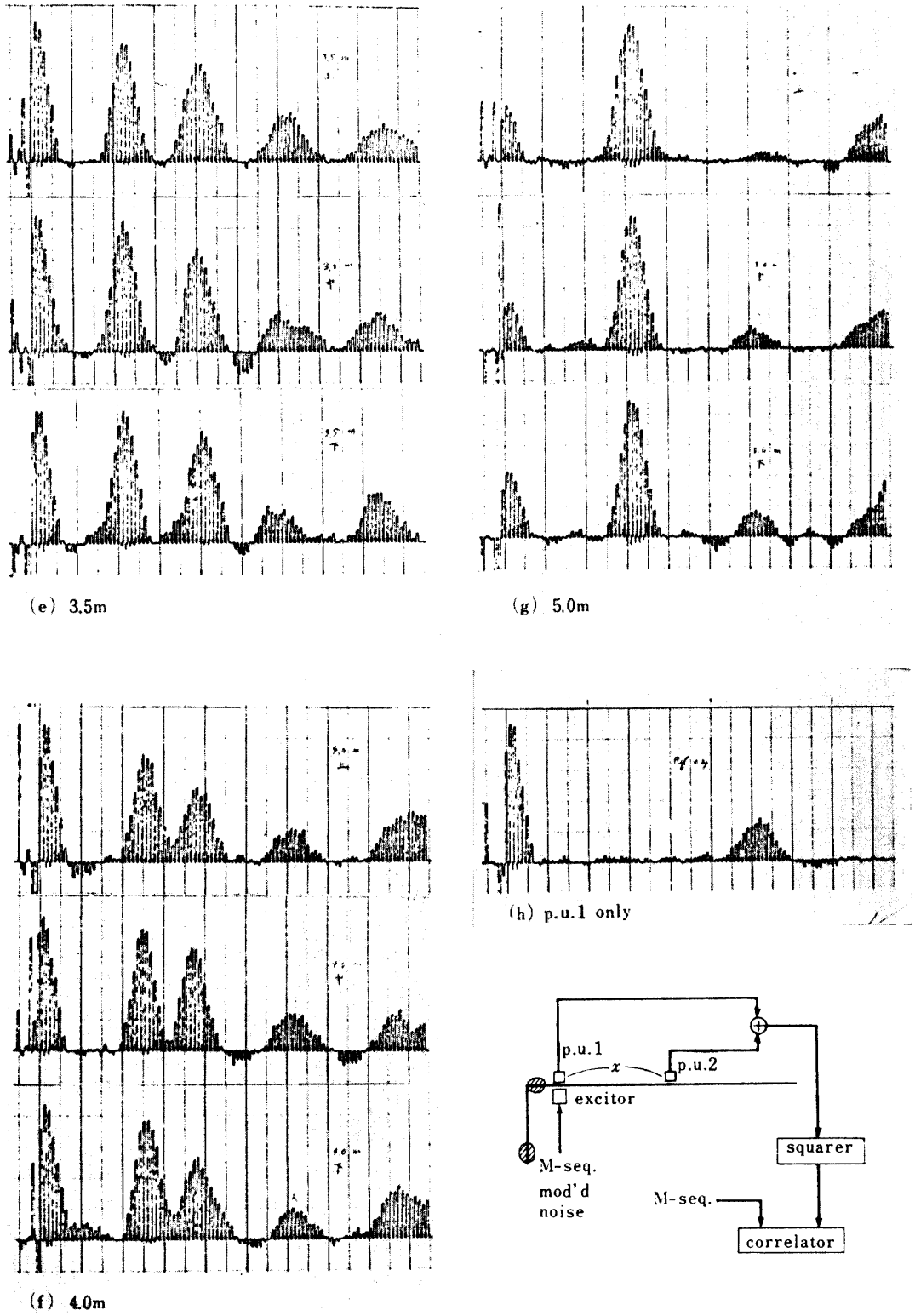

FIG. 16. Flexural wave reflection at the free end. 1 kHz 1/3 oct.

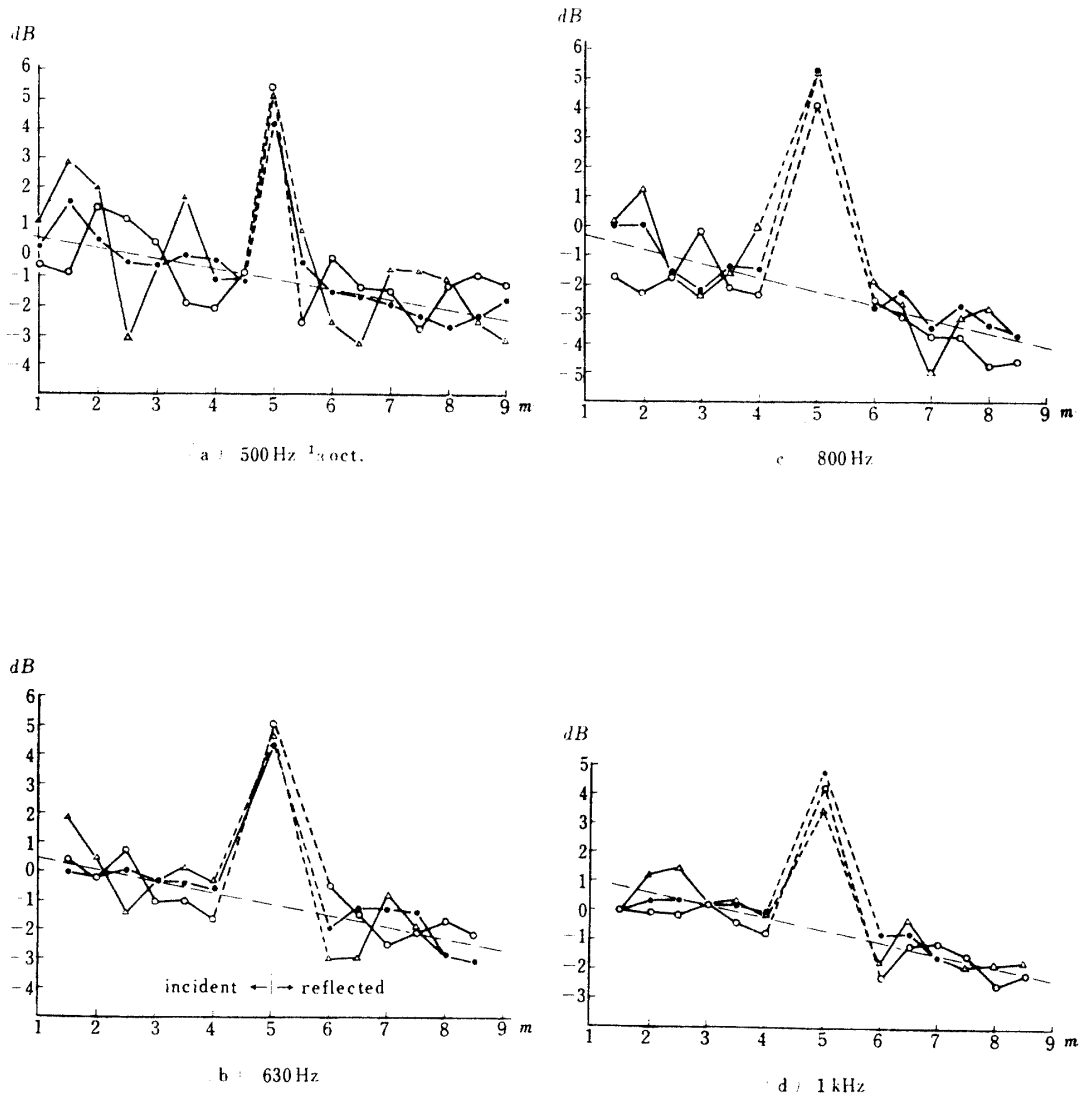

FIG. 17.

compaired with the velocity of longitudinal wave, the half of the incident wave is reflected and the other half is transmitted. The results of Fig. 18 show that the reflection is very small. One of the reasons is perhaps the roundness at the bend, which is about 1 cm radius. The spatial attenuation coefficient is difficult to obtain from these results.

In the two measurements described above, the signal frequency is restricted under 2 kHz. It is because at higher frequency, sometimes the low speed wave component which is hard to explain is observed. This phenomenon appears to the steel strip when the excitor is placed unsymmetrically and the pick-up is near the

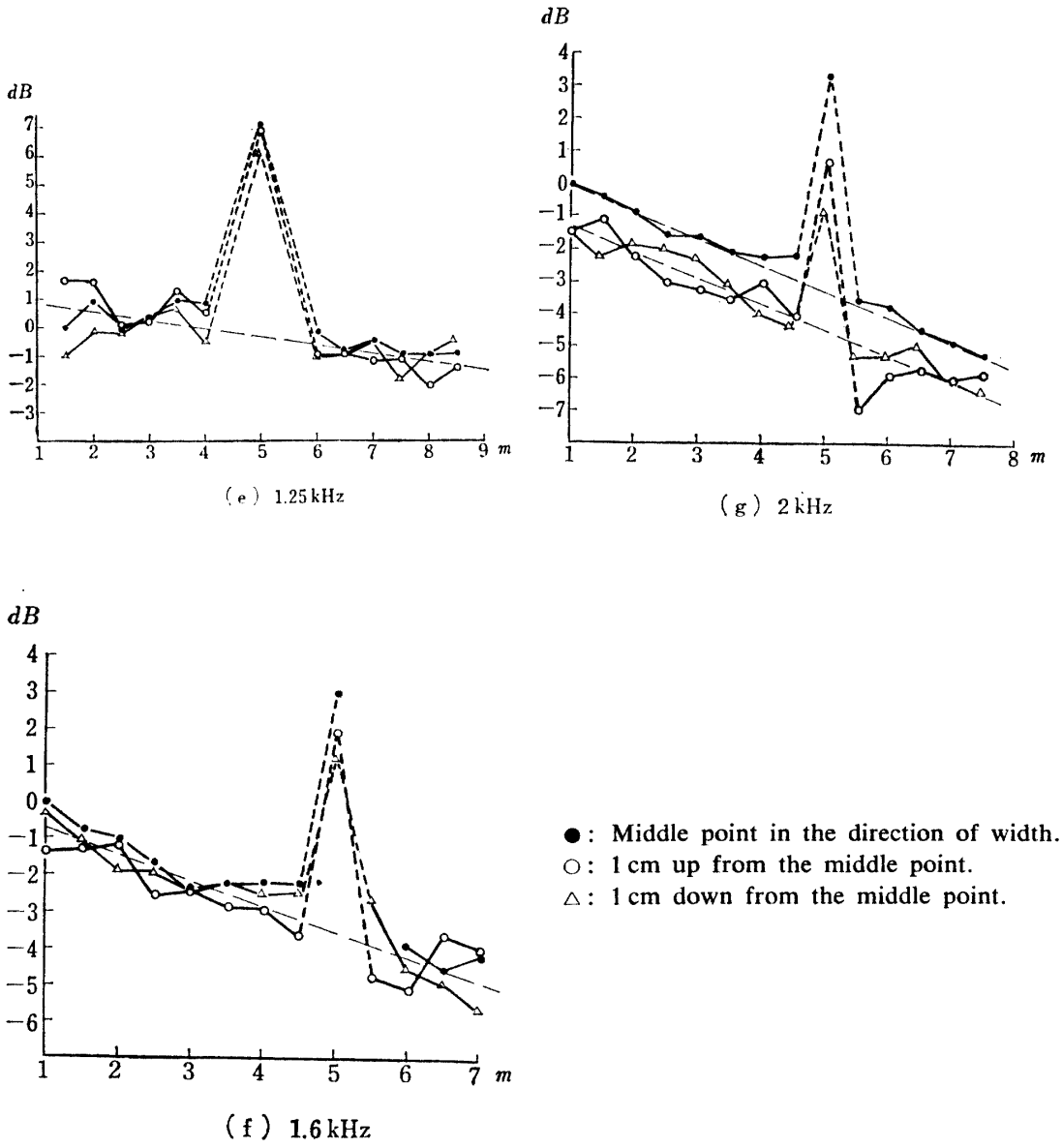

Fig. 17. Flexural wave reflection at the Free end.

center of the width. One of the examples is shown in Fig. 19. The free end of the strip is cut to form slant edge of 60°, and the excitor is placed parallel to the edge. The pick-up is placed at the center of width and moved up and down 1 cm apart from the center. Three measurements at each distance are grouped in Fig. 19, which shows that only at the center the long time delayed component appears, whose velocity is about 2/3 of the normal wave. Fig. 19 is the case of 3.15 kHz and at the frequencies 2.5–10 kHz, the same results are obtained. The tendency is observed that the difference between the normal and abnormal wave velocity decreases as the frequency increases. The measurements moving the pick-up in the

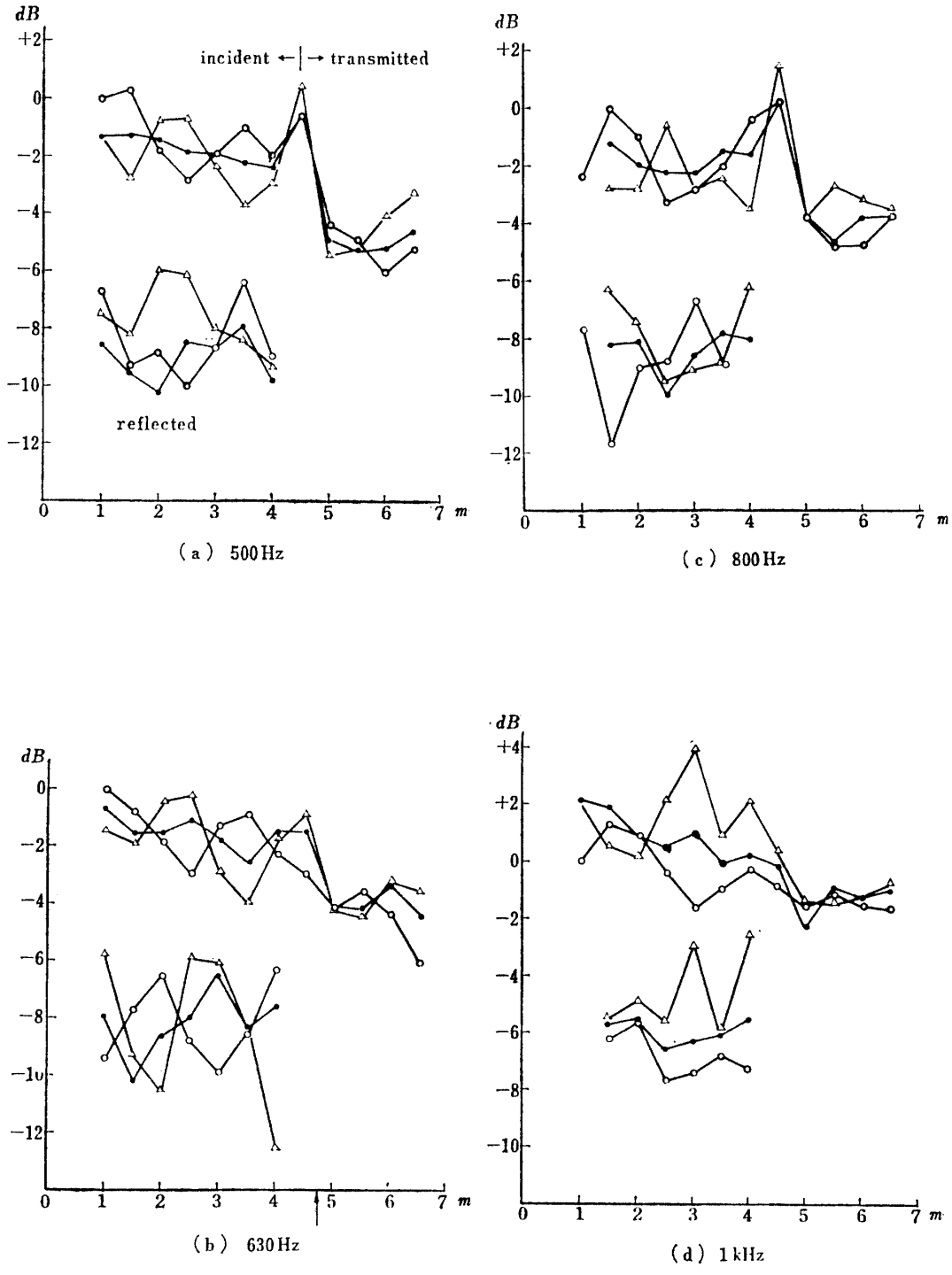

FIG. 18.

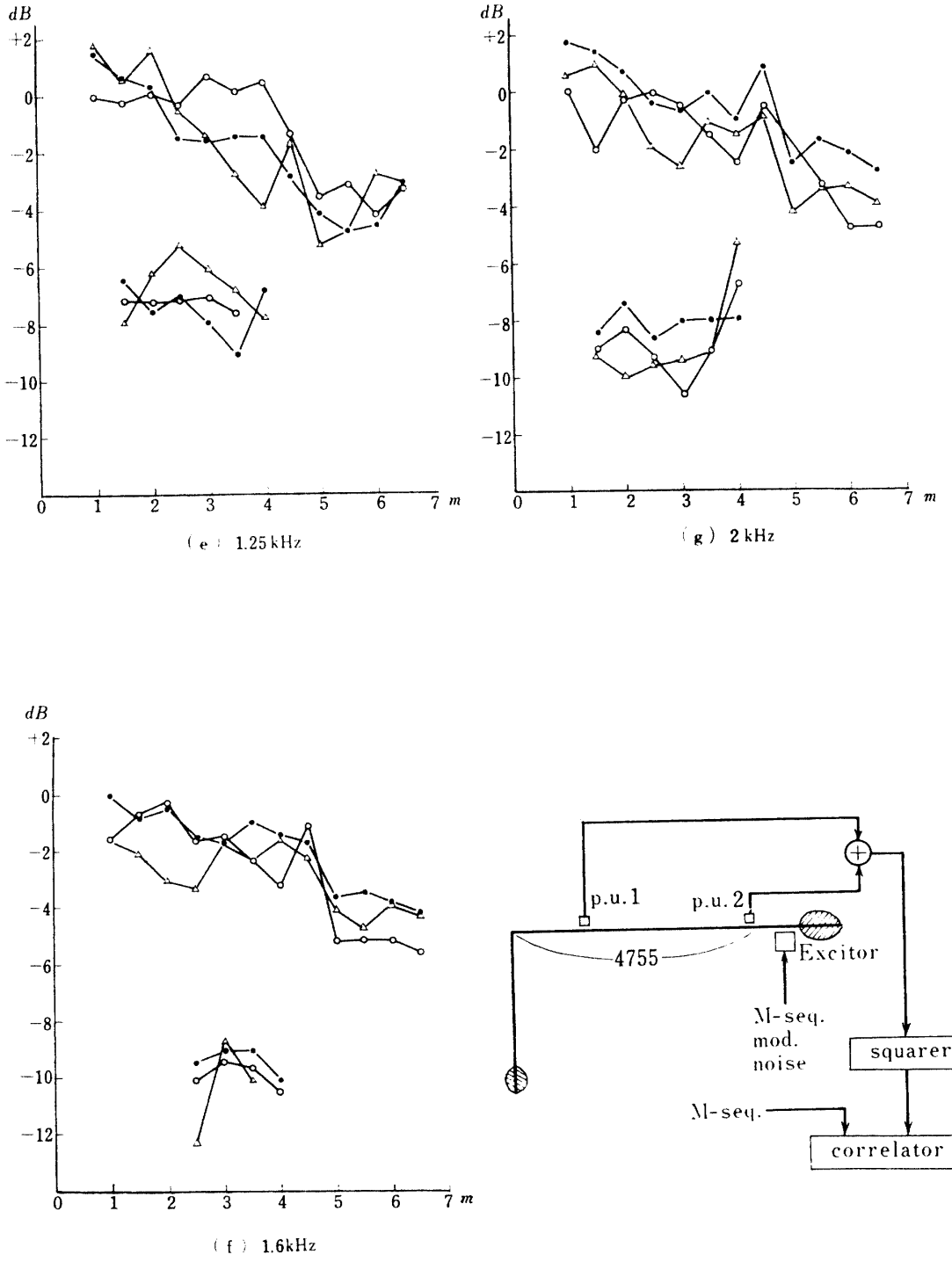

FIG. 18. Reflection and transmission at the bend.

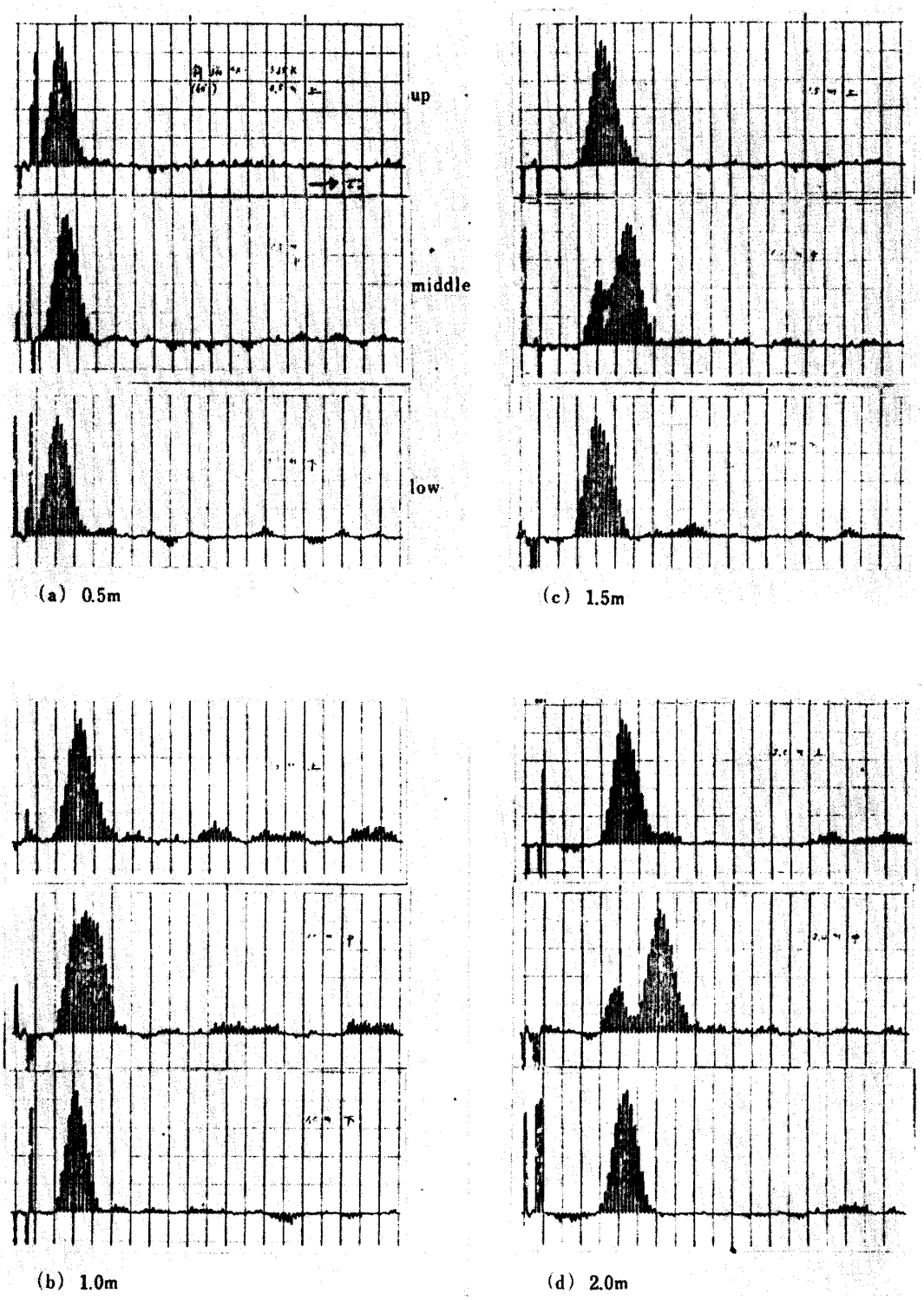

FIG. 19.

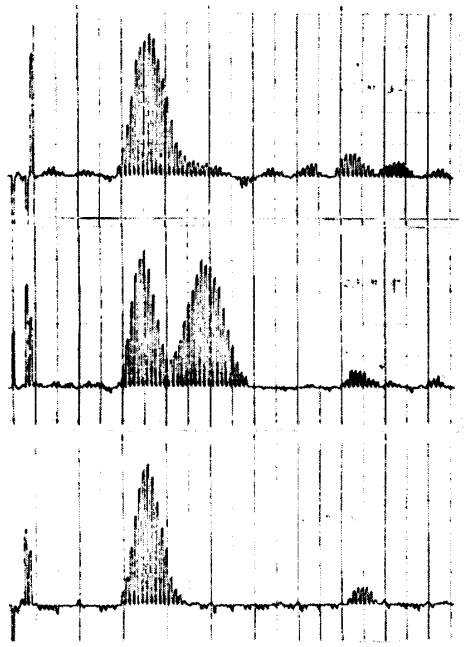

(e) 2.5 m

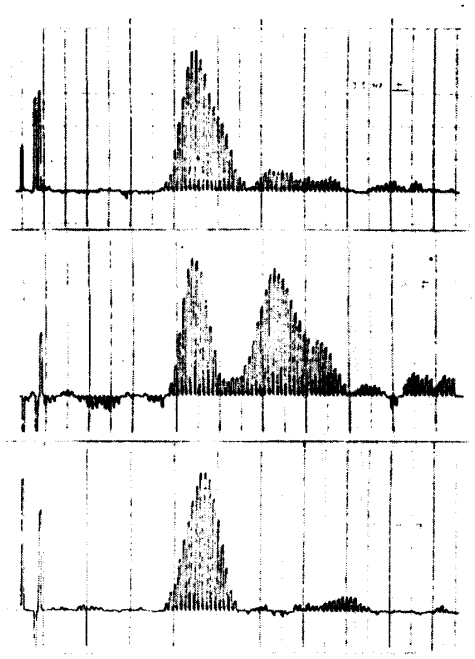

(g) 3.5m

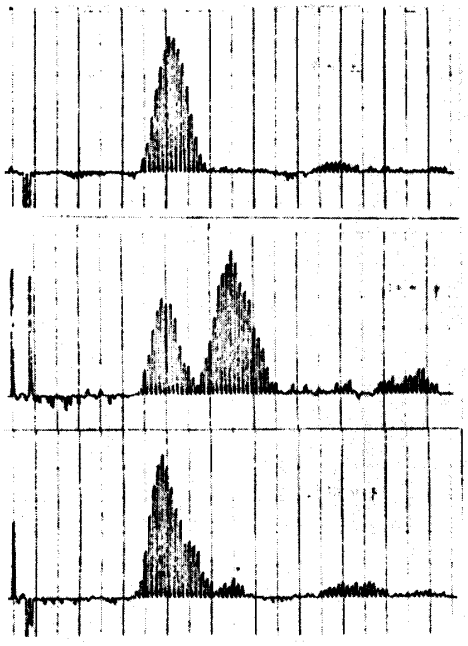

(f) 3.0m

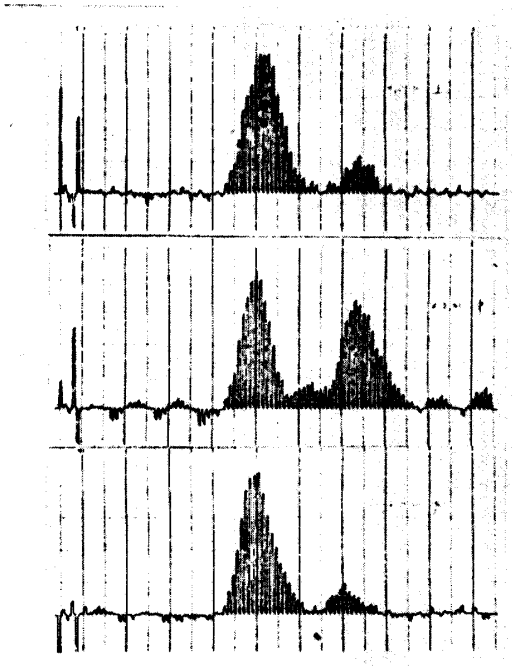

(h) 4.0m

FIG. 19.

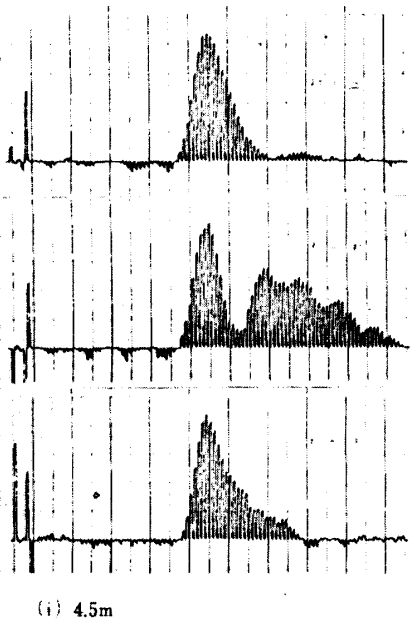

FIG. 19. Flexural wave excited at the slant edge. Abnormal component appears. 3.15 kHz. Three positions of each distance are grouped.

direction of width by 5 mm step are shown in Fig. 20. It is clearly seen that the abnormal component appears near the center. The exact explanation of these phenomena is not yet obtained.

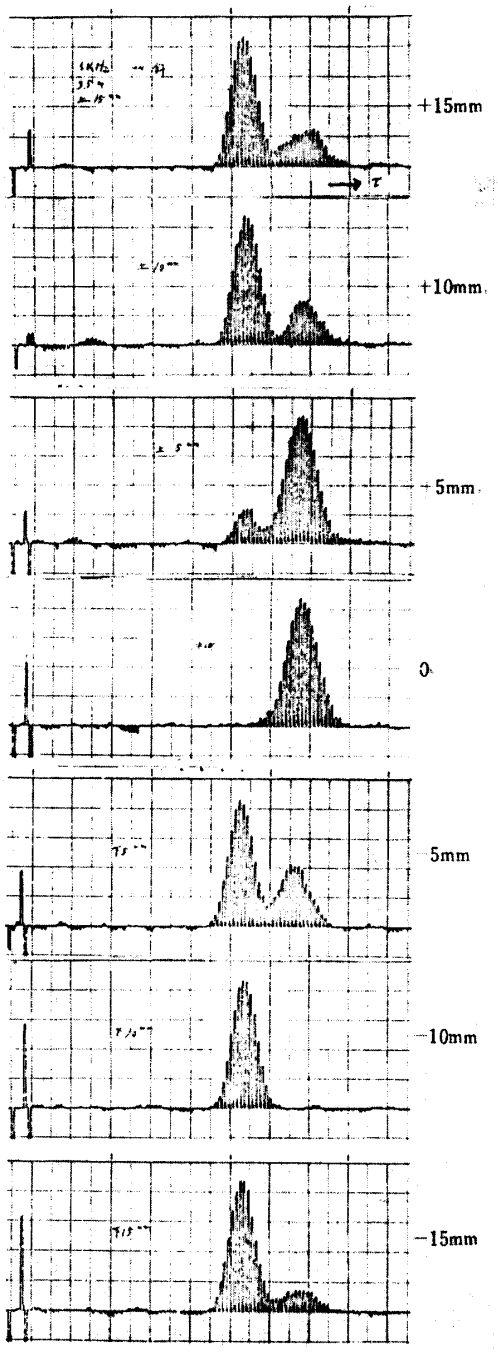

FIG. 20. Flexural wave excited at the slant edge. Pick-up is moved in the direction of width by 5 mm step. 5 kHz. 3.5 m from the excitor.

6. ACKNOWLEDGMENT

This study is made for the author's doctoral thesis in Graduate Course of Engineering, University of Tokyo. The author wishes to express great thanks for the guidance and the encouragement of Professor Juichi Igarashi. He is also indebted much to Dr. Yasushi Ishii, and thanks for Dr. Toshiyuki Ueno and Mr. Atsuo Fujisawa for their assistance and useful discussion.

Department of Instruments and Electronics
Institute of Space and Aeronautical Science
University of Tokyo, Tokyo
February 17, 1970

REFERENCES

[1] Kenneth W. Goff: The Application of Correlation Techniques to Some Acoustic Measurements, The Journal of the Acoustical Society of America, Vol. 27, No. 2, pp. 236–246, March 1955.

[2] T. Idogawa: Sound Velocity Measurement by Real-Time Correlation Methods, Transactions of the Society of Instrument and Control Engineers, Vol. 4, No. 1, pp. 69–76, March 1968 (in Japanese).

[3] N. Aoshima and J. Igarashi: M-sequence Signal Applied to the Correlation Measurement of Acoustical System, The Journal of the Acoustical Society of Japan, Vol. 24, No. 4, pp. 197–206, July 1968 (in Japanese).

[4] N. Aoshima and J. Igarashi: The Measurement of the Flexural Wave Propagation Velocity by Correlation Techniques, Report of the Institute of Space and Aeronautical Science, University of Tokyo, No. 436, March 1969.

[5] Leonard Meirovitch: Analytical Methods in Vibration, Macmillan, 1967.

[6] Y. Ishii *et al.*: An Electronic Real-Time Correlator, Reports of the 1967 spring meeting, The Accustical Society of Japan, p. 323, May 1967 (in Japanese).

[7] Y. Ishii: A Real-Time Signal Processing System for Correlation and Spectrum Analysis, Journal of the Society of Instrument and Control Engineers, Vol. 8, No. 11, pp. 734–749, November 1969 (in Japanese).

[8] L. Knopoff: Attenuation of Elastic Waves in the Earth, Physical Acoustics (edited by W. P. Mason) Volume 3–Part B, pp. 287–324, Academic Press, 1965.